Original

Staron, P.; Beckmann, F.; Lippmann, T.; Stark, A.; Oehring, M.; Pyczak, F.;
Salgado, M; Hort, N.; Eckerlebe, H.; Kainer, K.U.; Mueller, M.; Schreyer, A.:

In situ studies of light metals with synchrotron radiation and neutrons

Materials Science Forum, Light Metals Technology V (2011)
Trans Tech Publications

DOI: 10.4028/www.scientific.net/MSF.690.192

Materials Science Forum Vol. 690 (2011) pp 192-197

doi:10.4028/www.scientific.net/MSF.690.192

In situ studies of light metals with synchrotron radiation and neutrons

P. Staron[a], F. Beckmann[b], T. Lippmann[c], A. Stark[d], M. Oehring[e], F. Pyczak[f], M. Salgado[g], N. Hort[h], H. Eckerlebe[i], K.U. Kainer[j], M. Müller[k], A. Schreyer[l]

Institute of Materials Research, Helmholtz-Zentrum Geesthacht, 21502 Geesthacht, Germany

[a]Peter.Staron@hzg.de, [b]Felix.Beckmann@hzg.de, [c]Thomas.Lippmann@hzg.de, [d]Andreas.Stark@hzg.de, [e]Michael.Oehring@hzg.de, [f]Florian.Pyczak@hzg.de, [g]Mario.Salgado@hzg.de, [h]Norbert.Hort@hzg.de, [i]Helmut.Eckerlebe@hzg.de,

[j]Karl-Ulrich.Kainer@hzg.de, [k]Martin.Mueller@hzg.de, [l]Andreas.Schreyer@hzg.de

Keywords: X-ray diffraction; neutron diffraction; *in situ* studies; light metals

Abstract. High-energy X-rays and neutrons offer the large penetration depths that are often required for the determination of bulk properties in engineering material research. In addition, new sources provide very high intensities on the sample, which can be used not only for high spatial resolution using very small beams, but also for high time resolution in combination with a fast detector. This opens up possibilities for a wide range of specific engineering *in situ* experiments. Typical examples that are already widely used are heating or tensile testing in the beam. However, there are also more challenging experiments in the field of light metals, like e.g. friction stir welding, dilatometry, solidification, or cutting. Selected examples are presented.

Introduction

Neutron scattering is widely used in materials research involving diffraction, small-angle scattering, or tomography [1]. The corresponding techniques for investigation of texture, residual stress, precipitates, and other elements of the microstructure have been developed over decades and are still under development today. Available sample environments include, e.g., furnaces and load frames for *in situ* testing. Neutron experiments sometimes suffer from the low brilliance of the sources, and the design of sophisticated instruments for increasing the flux on the sample is a challenge. However, neutrons have unique properties (scattering power, magnetic moment, penetration depth, energy regime) making them indispensable not only for material research. The new European Spallation Source (ESS) will greatly improve the situation and enable flux-hungry experiments that were not possible before the advent of such sources [2].

X-ray scattering and micro-tomography using synchrotron radiation has evolved over the last decade as an increasingly utilized technique for characterizing the internal structure of materials. This development is based on the higher brilliance that synchrotrons offer, compared to laboratory X-ray sources, leading to an increased resolution in reciprocal and real space. Synchrotron sources can offer a wide energy spectrum, thus high energies (50–150 keV) can be used for achieving large penetration depth in light metals. The high brilliance of the source can be used for high spatial or time resolution, enabling experiments that are not possible with laboratory sources or neutrons. In general, both probes, neutrons and X-rays, can be regarded as complementary [3].

The Helmholtz-Zentrum Geesthacht utilizes both neutron and X-ray experiments for engineering material research [4]. New beamlines were built at the third generation synchrotron source PETRA III at DESY with an instrumentation that has a focus on *in situ* experiments [5]. The principal layout of a high-energy synchrotron experiment is sketched in Fig. 1. The scattering angles are small at high X-ray energies so that complete Debye-Scherrer rings can be recorded with an area detector [6]. When the area detector is placed several meters away from the sample, also small-angle scattering can be recorded. The beam size can vary between 0.01 and 1 mm; sub-micron beams can be produced by focussing X-ray lenses. Closed sample environments with vacuum or shielding gases are built with beam windows.

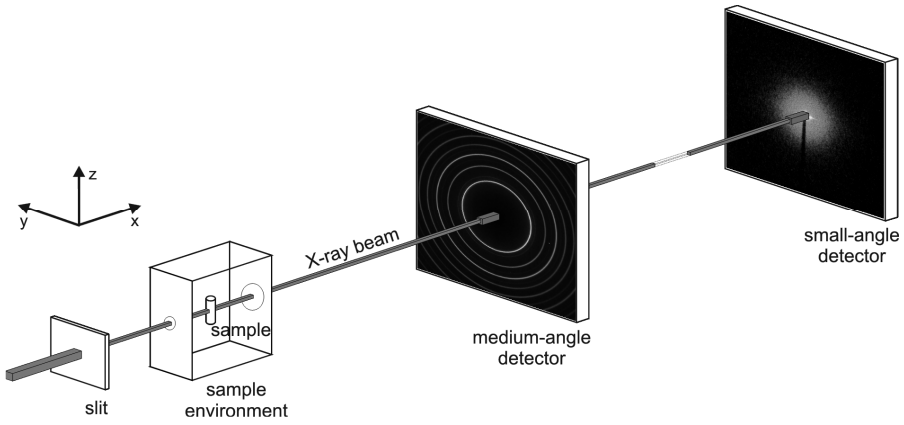

Fig. 1: Sketch of an experiment using high-energy X-rays. An area detector can be placed close to the sample (≈1 m) for recording Debye-Scherrer rings, or far away from the sample (≈10 m) for recording small-angle scattering.

In situ experiments require special sample environments applying specific environmental conditions to the sample. These cover all sorts of heating and cooling, application of mechanical forces or different fields or media. The challenge is to combine a complex and bulky sample environment with the need to feed the neutron or X-ray beam through it. Sometimes neutrons are advantageous for this purpose because they enable large scattering angles, sometimes high-energy X-rays are advantageous because of their small scattering angles. Another requirement is fast detectors for kinetic studies.

One example for successful *in situ* experiments at the HZG beamlines at DESY is a transportable machine for *in situ* friction stir welding experiments with a state-of-the-art welding head. Another example is an *in situ* cutting experiment, where the formation of cutting chips was studied [7]. *In situ* experiments with a dilatometer will be introduced in the following. A special challenge for *in situ* tomography experiments is the need for a precise rotation of the sample for 180°, which must not be hindered by the sample environment. Moreover, this rotation needed for one tomogram has to be fast enough to follow the sample kinetics. This requires high flux, a fast detector, and stable mechanics. The second example shows investigations where also *in situ* tomography and diffraction experiments dealing with the solidification of Mg alloys are planned. Finally, the investigation of isothermal precipitation kinetics in Al alloys using *in situ* small-angle neutron scattering is introduced.

The transformation mechanism of ternary phases in Nb-rich γ-TiAl alloys

Intermetallic γ-TiAl based alloys are a class of novel, lightweight structural materials with attractive mechanical properties for advanced high-temperature applications. Conventional titanium aluminides are two-phase alloys consisting of tetragonal γ-TiAl and small amounts of hexagonal α_2-Ti_3Al. Due to their low density, their high yield and creep strength up to 800 °C, and their good oxidation resistance they are used to replace heavier Ni-based superalloys in industrial and in aviation gas turbines as well as in automobile engines [8]. However, their low ductility impedes broad industrial application up to now. Recently, intermetallic γ-TiAl based alloys with additional amounts of the ternary bcc β-Ti(Al) phase attracted increasing attention due to their improved workability at elevated temperatures [9, 10, 11, 12]. Depending on alloy composition and heat treatment, the ductile high-temperature β phase can transform to several ordered phases at lower temperatures. However, actually available phase diagrams of these multiphase alloys are quite uncertain and the precipitation kinetics of some metastable phases is far from understood.

Thus, *in situ* high-energy X-ray diffraction experiments were performed at the HZG beamline HARWI II at Deutsches Elektronen-Synchrotron (DESY) [13]. At a photon energy of 100 keV (λ = 0.12398 Å) the resulting diffraction rings were recorded on a Mar555 flat panel detector each 120 s with an exposure time of 20 s. The highest possible frame rate with that detector is 0.37 s^{-1}, but also significantly faster detectors exist.

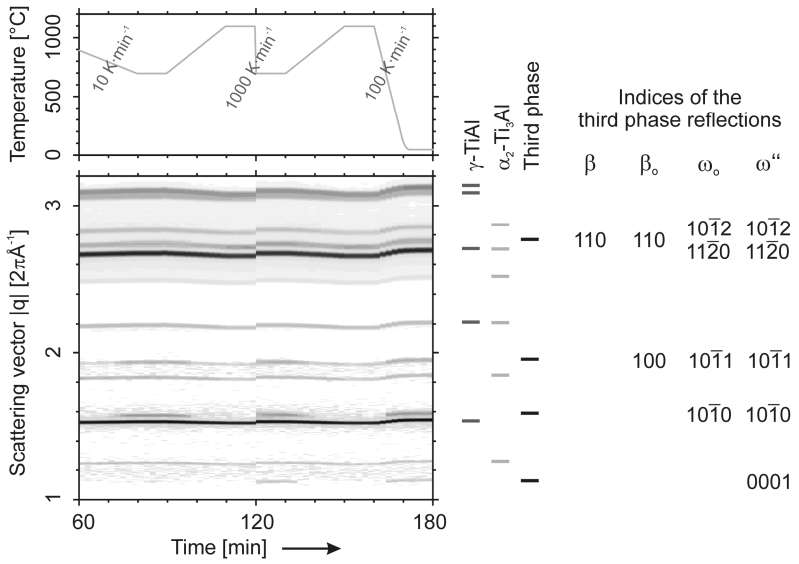

Fig. 2: Temperature ramp and development of the diffraction pattern with time [13]. The pattern intensity is coded in grey scale; $|\mathbf{q}| = 2\pi/d = 2\pi\cdot(2\sin\theta/\lambda)$. Gain and contrast of the weak super-structure reflections are increased. The illustration starts in the first cooling cycle at $t = 60$ min.

A commercial dilatometer DIL 805A/D (Bähr-Thermoanalyse GmbH) with modifications for working in the synchrotron beam was used for heating and quenching of samples with a diameter of 4 mm [5]. The samples were heated up to 1100 °C and subsequently quenched to 700 °C with quenching rates of 10, 1000 and 100 $K\cdot min^{-1}$.

Depending on the quenching rate, reversible transformations of the cubic B2-ordered β_o phase to different ω related phases are observed in Ti-45Al-10Nb (Fig. 2). At low quenching rates the hexagonal $B8_2$-ordered ω_o phase is formed while at high quenching rates the metastable intermediate trigonal ω'' phase can be preserved. The results indicate that the complete transformation $\beta_o \rightarrow \omega_o$ consists of the steps $\beta_o \rightarrow$ ω'' and ω'' $\rightarrow \omega_o$, which are both diffusion controlled. The transformation step $\beta_o \rightarrow$ ω'' only needs atomic rearrangements over relative short distances which can occur significantly faster than the diffusion processes necessary for the ω'' $\rightarrow \omega_o$ transformation.

With the modified commercial dilatometer in the synchrotron beam, elongation and phase content can be measured simultaneously during precise and fast heat treatments. Moreover, installations of a deformation as well as a DSC unit are options to expand the measurement possibilities. This makes the dilatometer a unique sample environment for *in situ* materials research experiments.

Microstructure analysis of Mg alloys by micro-tomography

Mg-alloys represent a suitable alternative for lightweight parts in the automotive and aeronautic industries. Therefore, the study of Mg-alloy solidification is an important issue for the optimization of manufacturing processes. The solidification of metals is a complex process that starts with the nucleation of a solid embryo in an under-cooled region of a liquid melt, proceeds with the growth of a primary solid phase, and ends with the precipitation and growth of secondary phases [14, 15]. Most of the experimental evidence to explain these mechanisms relies on static or *ex situ* studies of as-cast specimens. However, some further questions on how a microstructure reaches its final state and how such a process can be controlled on behalf of the final properties of the material can only be addressed through *in situ* characterization techniques.

With 3rd generation Synchrotron light sources (e.g. PETRA III at DESY) it is possible to perform *in situ* X-ray diffraction, radiography, and tomography experiments to study the physical phenomena associated with the solidification of metals. Up to present, only a few X-ray synchrotron tomography studies of as-cast and extruded microstructures of commercial Mg-alloys have been performed [16, 17] in order to investigate the size, morphology and distribution of primary and secondary phases after processing. As an example, tomography experiments at room temperature

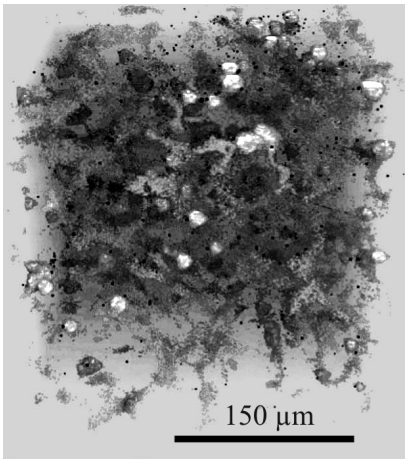

Fig. 3: 3-D segmented β phase (grey), micro-pores (black dots) and Al–Mn phases (white) in an as-cast AZ91D as obtained from µCT [17].

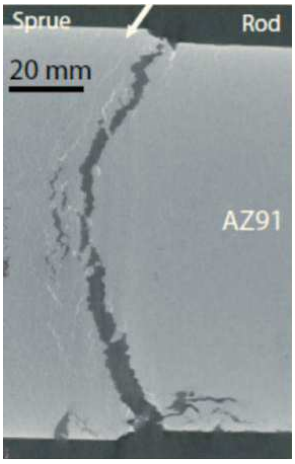

Fig. 4: Crack volume for an AZ91 alloy solidified in a sprue-rod mould (mould temperature = 200 °C, crack volume = 52 mm^3).

[17] have allowed to compare the microstructures of as-cast and extruded alloys, and investigate the amount, size, and distribution of intermetallic phases in the interdendritic regions. Fig. 3 shows the distribution of the secondary phases $Mg_{17}Al_{12}$ and Al_5Mn_8 of an as-cast AZ91 specimen. Also the presence of micro-porosity can be identified. A resolution of 1.5 µm was achieved for cylindrical specimens having 2 mm diameter.

The formation and growth of hot cracks during the last stages of solidification is another problem not fully understood. This defect is induced by tensile stresses acting within regions of a solidifying specimen that still remains at high solid fractions. These tensile stresses are a direct consequence of the cooling conditions and the geometry of the specimen. Mg alloys are not exempt of presenting hot cracks, and these have been recognized in particular on Mg alloys of the AZ series [18, 19]. A first approach to understanding hot cracking in binary Mg-Al and Mg-Zn alloys is the sprue rod test [20]. The hot cracks induced during solidification of an AZ91 alloy solidified with initial mould temperature of 200 °C was further characterized through X-ray computer-based tomography (Fig. 4). The corresponding crack volume was quantified through a small routine developed with the software 'ImageJ'. An additional advantage of this method is that the complete crack morphology can be investigated. *In situ* tomography experiments are also planned for the future, because only *in situ* studies can reveal the kinetics of phase or crack formation. For this purpose, a specially designed two-zone furnace is constructed, which is able to maintain a thermal gradient along the specimen, and which can be rotated to allow for tomography. Moreover, also nano-tomography at PETRA III will be applied, which yields information with spatial resolutions down to <100 nm.

Precipitation kinetics in AA60xx Al alloys

Small-angle neutron scattering (SANS) is a classical method for the study of precipitation kinetics in alloys [21]. With standard SANS instruments, precipitate size distributions in the range of about 1–100 nm can be determined. When the chemical compositions of matrix and precipitates are known, also precipitate volume fractions can be determined. The advantage of SANS is the sensitivity for small changes in the size distribution because a relatively large sample volume of about 0.1 cm^3 can be probed. Thus, SANS is ideally combined with transmission electron microscopy (TEM) and atom probe (3DAP), for which the field of view is very small.

Age-hardenable Al alloys play an important role in aircraft construction. Existing alloys are modified and new alloys are developed to improve, e.g., strength and fatigue properties according to increasing demands. Such alloys are strengthened by second-phase precipitates with sizes of a few nanometres. Thus, small-angle scattering is ideally suited for the characterization of these precipitates. The precipitation kinetics at aging temperature can be studied *in situ* with a furnace in

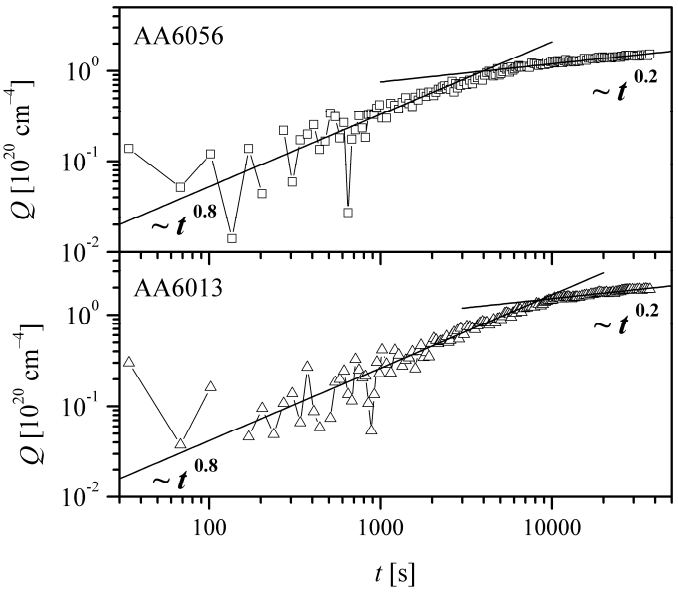

Fig. 5: Integrated SANS intensity as a function of aging time at 190 °C for two different Al alloys of the AA60xx series. The first data point was taken 30 s after T = 190 °C was reached.

the beam. When X-rays from a synchrotron source are used for such studies, very high time resolution can be achieved because of the high intensity. However, some alloys do not have a significant contrast between matrix and precipitates and the small-angle X-ray scattering (SAXS) signal is negligible. Nevertheless, such alloys can still be studied with SANS because the scattering contrast for neutrons is completely different.

This is also the case for the Al alloy AA6056. The precipitates contain Mg and Si so that no SAXS signal was observed. SANS, however, produced a strong signal. SANS measurements had been carried out at the instrument SANS-2 of the Helmholtz-Zentrum Geesthacht. The mean neutron wavelength was 0.58 nm, the detector distance was 1 m. A furnace with ceramic heating elements in close contact with the sample was used for the experiment [22]. The aging temperature of 190 °C was reached within 13 s so that early stages of the isothermal reaction could be observed. The data acquisition time in this stage was 30 s, giving rather weak statistics. Thus, the integrated intensity Q was calculated, which is proportional to the precipitate volume fraction and the scattering contrast. When the chemical composition of the precipitates does not change, e.g. in the case of classical nucleation and growth, and the covered range of scattering vectors is large enough, Q is a measure for the precipitate volume fraction.

Two stages could be distinguished in the precipitation reaction at 190 °C: in the beginning, Q grows with $t^{0.8}$, while after about 2 hours Q grows with $t^{0.2}$ (Fig. 5). The mean precipitate radius grows to about 2.5 nm in the observed time range. The alloy AA6013 with a slight variation in the composition shows a very similar behaviour. The further evaluation of the SANS data includes the determination of precipitate sizes as a function of isothermal aging time; the results will be published elsewhere.

Such data can only be produced by small-angle scattering techniques. The statistics and time resolution of the presented SANS measurements can still be significantly improved by using neutron sources stronger than a medium-flux reactor, such as FRM II [23] or ESS [2]. The results can help to improve the understanding of details of the precipitation reaction, either by direct evaluation or by comparison with model predictions. In this way, they can also contribute to the improvement of mechanical properties of such materials and the development of alloy modifications.

Outlook

The unprecedented brilliance of third-generation synchrotron sources like PETRA III and the unprecedented flux of spallation neutron sources like ESS enable new *in situ* experiments with extremely high spatial and time resolution. This opens up new possibilities for investigations of microstructural elements and technical processes in the field of engineering materials research.

Acknowledgement

W.V. Vaidya from HZG is gratefully acknowledged for providing the Al alloys for the SANS measurements.

References

[1] W. Reimers, A.-R. Pyzalla, A. Schreyer, H. Clemens (eds.): *Neutrons and synchrotron radiation in engineering materials science*, Wiley VCH, Weinheim (2010).
[2] http://www.esss.se
[3] A. Pyzalla, W. Reimers, K.-D. Liss, Mater. Sci. Forum 347–349 (2000) 34–39.
[4] P. Staron, N. Schell, A. Haibel, F. Beckmann, T. Lippmann, L. Lottermoser, J. Herzen, T. Fischer, M. Koçak , A. Schreyer, Mater. Sci. Forum 639–642 (2010) 2470–2475.
[5] P. Staron, T. Fischer, T. Lippmann, A. Stark, S. Daneshpour, D. Schnubel, E. Uhlmann, R. Gerstenberger, B. Camin, W. Reimers, E. Eidenberger, H. Clemens, N. Huber, A. Schreyer, Adv. Eng. Mater., DOI: 10.1002/adem.201000297.
[6] K.-D. Liss, A. Bartels, A. Schreyer, H. Clemens: Textures Microstruct. 35 (2003) 219.
[7] E. Uhlmann, R. Gerstenberger, S. Herter, T. Hoghé, W. Reimers, B. Camin, R.V. Martins, A. Schreyer, T. Fischer, Prod. Eng. Res. Devel. 5 (2010) 1–8.
[8] Y.-W. Kim, D. Morris, R. Yang, C. Leyens (eds.): *Structural Aluminides for Elevated Temperature Applications*, TMS, Warrendale, PA, USA (2008).
[9] M. Takeyama, S. Kobayashi: Intermetallics 13 (2005) 993.
[10] F. Appel, M. Oehring, J.D.H. Paul: Adv. Eng. Mater. 8 (2006) 371.
[11] H. Clemens, W. Wallgram, S. Kremmer, V. Güther, A. Otto, A. Bartels: Adv. Eng. Mater. 10 (2008) 707.
[12] K.-D. Liss, T. Schmoelzer, K. Yan, M. Reid, M. Peel, R. Dippenaar, H. Clemens: J. Appl. Phys. 106 (2009) 113526.
[13] A. Stark, M. Oehring, F. Pyczak: Proc. MRS 2010 Fall Meeting, Boston, MA.
[14] W. Kurz, D.J. Fisher: *Fundamentals of Solidification*, Trans Tech Publications, Switzerland, 4th edition (1998).
[15] J.A. Dantzig, M. Rappaz: *Solidification*, EPFL Press, Distributed by CRC Press (2009).
[16] S.B. Yi, H.-G. Brokmeier, R.E. Bolmaro, K.U. Kainer, T. Lippmann: Scripta Mater. 51 (2001) 455–460.
[17] F. Witte, J. Fischer, F. Beckmann, M. Störmer, N. Hort: Scripta Materialia 58 (2008) 453–456.
[18] P. Gunde, A. Schiffl, P.J. Uggowitzer: Mater. Sci. and Eng. A 527 (2010) 7074–7079.
[19] K. Hu, A.B. Phillion, D.M. Maijer, S.L. Cockcroft: Scripta Mater. 60 (2009) 427–430.
[20] Z.S. Zhen, N. Hort, Y.D. Huang, O. Utke, N. Petri, K.U. Kainer: Int. Journal Cast Met. Res. 22 (2009) 331–334.
[21] G. Kostorz, in: Treatise on Materials Science and Technology, Vol. 15: Neutron Scattering, G. Kostorz, H. Herman (eds.), Academic Press, New York (1979) 227–289.
[22] P. Staron, E. Eidenberger, M. Schober, M. Sharp, H. Leitner, A. Schreyer, H. Clemens, J. Physics: Conf. Series 247 (2010) 012038.
[23] http://www.frm2.tu-muenchen.de